Research Article

Anthropogenic Carbon Nanotubes Found in the Airways of Parisian Children

CrossMark

Jelena Kolosnjaj-Tabi [a], Jocelyne Just [b], Keith B. Hartman [c], Yacine Laoudi [b], Sabah Boudjemaa [d], Damien Alloyeau [e], Henri Szwarc [a], Lon J. Wilson [c,*], Fathi Moussa [a,f,**]

[a] LETIAM, Lip(Sys)², IUT d'Orsay, Paris-Saclay University, Plateau de Moulon, 91400 Orsay, France
[b] Paediatric Pulmonology and Allergy Center, Trousseau-La Roche Guyon Hospital group, Assistance Publique — Hôpitaux de Paris, Pierre et Marie Curie-Paris 6 University, Paris, France
[c] Department of Chemistry, Richard E. Smalley Institute for Nanoscale Science and Technology, P.O. Box 1892, Rice University-MS 60, Houston, TX 77251-1892, USA
[d] Department of Anatomo-pathology, Trousseau-La Roche Guyon Hospital group, Assistance Publique — Hôpitaux de Paris, Pierre et Marie Curie-Paris 6 University, Paris, France
[e] Laboratoire Matériaux et Phénomènes Quantiques, UMR 7162, CNRS - Université Paris Diderot, Paris, France
[f] Department of Biochemistry, Trousseau-La Roche Guyon Hospital group, Assistance Publique — Hôpitaux de Paris, Pierre et Marie Curie-Paris 6 University, Paris, France

ARTICLE INFO

ABSTRACT

Compelling evidence shows that fine particulate matters (PMs) from air pollution penetrate lower airways and are associated with adverse health effects even within concentrations below those recommended by the WHO. A paper reported a dose-dependent link between carbon content in alveolar macrophages (assessed only by optical microscopy) and the decline in lung function. However, to the best of our knowledge, PM had never been accurately characterized inside human lung cells and the most responsible components of the particulate mix are still unknown. On another hand carbon nanotubes (CNTs) from natural and anthropogenic sources might be an important component of PM in both indoor and outdoor air.

We used high-resolution transmission electron microscopy and energy dispersive X-ray spectroscopy to characterize PM present in broncho-alveolar lavage-fluids (n = 64) and inside lung cells (n = 5 patients) of asthmatic children. We show that inhaled PM mostly consist of CNTs. These CNTs are present in all examined samples and they are similar to those we found in dusts and vehicle exhausts collected in Paris, as well as to those previously characterized in ambient air in the USA, in spider webs in India, and in ice core. These results strongly suggest that humans are routinely exposed to CNTs.

© 2015 Published by Elsevier B.V. This is an open access article under the CC BY-NC-ND license (http://creativecommons.org/licenses/by-nc-nd/4.0/).

1. Introduction

At the dawn of the 21st century air pollution remains a growing public health threat (Lim et al., 2013), regardless of the fact that air quality should be regarded as an integral part of human rights (Samet and Gruskin, 2014). Among air pollutants, fine particulate matters (PMs) of less than 2·5 μm in diameter ($PM_{2.5}$) were recently ranked as one of the leading causes of death and disability worldwide (Lim et al., 2013). Recent studies indicate the persistence of adverse health effects and associate long-term exposure to $PM_{2.5}$ with natural-cause mortality even within concentrations below those recommended by the WHO and European institutions (Beelen et al., 2014). According to epidemiological studies, long-term exposure to high concentrations of PM increases the risk of cardiovascular (Pope et al., 2009; Shah et al., 2013)

and respiratory disease (Zemp et al., 1999), diabetes (Li et al., 2014) and lung cancer (Raaschou-Nielsen et al., 2013), whereas short-term exposure can exacerbate and/or onset various forms of respiratory disease, such as asthma (Guarnieri and Balmes, 2014; Gordon et al., 2014; Smith et al., 2000).

A recent review discussed clinical implications, policy issues, and research gaps relevant to air pollution and asthma (Guarnieri and Balmes, 2014). One of the most challenging tasks for air pollution research has been how to address the fact that people are almost always exposed to a mixture of pollutants (Kelly and Fussell, 2012). Concerning exposure to $PM_{2.5}$ the authors note that the most responsible components of the particulate mix are not known and they add that unraveling which components of the traffic pollution mixture are responsible for asthma exacerbations and onset is a substantial challenge (Guarnieri and Balmes, 2014). Obviously, this discussion may also apply to other adverse health effects such as cardiovascular disease and lung cancer.

Among particulate constituents, carbon, found in alveolar macrophages (AM), has been linked in a dose dependent manner to the decline in lung function (Kulkarni et al., 2006). In addition, a recent

* Corresponding author.
** Correspondence to: F. Moussa, LETIAM, Lip(Sys)², IUT d'Orsay, Paris-Saclay University, Plateau de Moulon, 91400 Orsay, France.
E-mail addresses: durango@rice.edu (L.J. Wilson), fathi.moussa@u-psud.fr (F. Moussa).

study suggested a possible mechanism underlying the observation that traffic-derived air pollution adversely affects children with asthma, because they may be less able to clear inhaled PM effectively (Brugha et al., 2014). In both studies, macrophage carbon content was assessed with image analysis of black material present inside AM, visualized with optical microscopy alone. Yet, based on empirical evidence, we postulate that lamellar bodies and carbon content cannot be distinguished by optical microscopy, and even low magnification transmission electron microscopy (TEM) because their sizes and aspects are quite similar. Hence, in order to unravel which components of carbonaceous PM are responsible for adverse effects, it is first important to thoroughly and specifically characterize the components present in the "black material inside AM".

In order to evaluate if PMs have been inhaled after environmental exposure, it is necessary to investigate for PM presence in the lungs of healthy subjects, which is elusive. In theory, it is possible to check for PM presence in organs during autopsy, but this cannot provide direct evidence of routine exposure, since their presence could result from previous accidental exposures.

The main objective of this work is to characterize the carbonaceous PMs found in the lungs of Parisian children. To attain this objective we used transmission electron microscopy (TEM), high-resolution TEM (HRTEM), energy dispersive X-ray spectroscopy (EDX), Raman spectroscopy, and near infrared fluorescence microscopy (NIRFM) to characterize PM. Our purpose was to find the most appropriate method to characterize PM.

Particulate matter was characterized in broncho-alveolar lavage fluid (BALF) extracts and *in situ* in AM of asthmatic Parisian children. Asthmatic patients, rather than healthy subjects, were selected for the study since fiber-optic bronchoscopy with broncho-alveolar lavage is routinely performed in France as a diagnostic tool for other missed diseases with symptoms similar to asthma (Just et al., 2002). Obviously, such an invasive method is ethically difficult to consider for healthy subjects.

2. Methods

2.1. Study Design and Sample Collection

The study was conducted on 69 randomly selected BALF residues collected from asthmatic infants and children living in Parisian area who had undergone treatment by the Pediatric Pulmonology and Allergy Center of Paris. BALF samples were obtained during fiber-optic bronchoscopy as part of normal clinical management with written informed consent of the parents of every subject. This study using only BALF residues was performed according to French public health regulations (*Code de la santé publique — Article L1121-3, modified by Law n°2011–2012, December 29 2011 — Article 5*).

We first retrospectively studied 64 BALF samples (36 boys and 28 girls aged between 2 to 204 months (17 years), median 54 months), randomly selected from a collection of BALF residues (frozen at Trousseau Hospital, Paris, France) collected between 2007 and 2011 from subjects with symptoms of unusual asthma (i.e. recurrent or persistent wheezing and resistance to high doses of inhaled corticosteroids). As freezing lysed the cells, we later analyzed five freshly collected BALF samples with intact airway cells from five randomly selected patients (males, aged 12 to 58 months, median age 23 months) with symptoms of unusual asthma. Macroscopic inflammation was observed in all five patients. Hypercellularity in BALF samples (>22 × 10⁴ cells/mL), mainly represented by AM and alveolar neutrophils, was present in four samples.
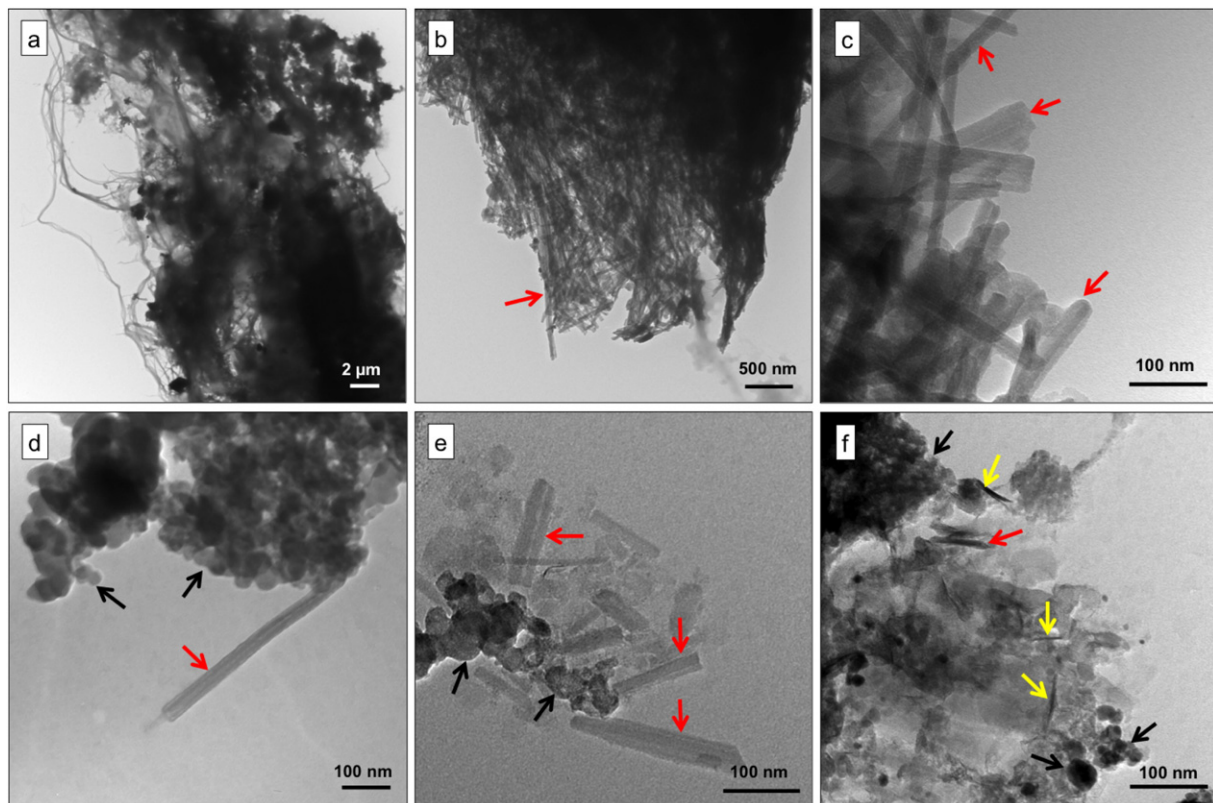

Fig. 1. TEM micrographs of BALF and dust extracts. (a, b) BALF extracts. (c) Magnified view of (b). (d) PM from vehicle exhausts showing carbon nanospherules (black arrows) and CNT-like structures (red arrows). (e, f) PM from dust deposited near a busy traffic intersection in the Parisian area showing nanospherules and CNT-like bundles (yellow arrows). Note the similarity between the CNT-like structures observed in (d, e) and (c).

2.2. Fiber-Optic Bronchoscopy With Bronchoalveolar Lavage (FBBAL)

FBBAL was performed under mild sedation and local anesthesia as previously reported (Just et al., 2002). The first BALF aliquot was processed for quantitative bacterial culture. Three other aliquots were pooled and processed for differential cell counting after Diff-Quick staining. The fifth aliquot was frozen and stored at −20 °C (for the first 64 analyzed BALF samples) or immediately processed (last five patients) for PM characterization.

2.3. PM Extraction and Concentration From BALF Samples

The extraction procedure has been performed as previously described (Kolosnjaj-Tabi et al., 2010) with minor modifications. Briefly, frozen BALF samples were unfrozen and centrifuged (3000 g/30 min) and pellets were mixed with 4 mL of distilled water. The mixture was vortexed for 2 min, stirred for 12 h, then subjected to alternative sonication (15 min) and vortexing (2 min, five times). After centrifugation, the pellet was prepared for TEM examination by re-dispersion in 200 μL of purified water with sonication for 10 min. 3 μL of the resulting suspension was deposited onto an ionized 400 mesh formvar-carbon-supported copper grid or an amorphous silicon-coated TEM grid.

2.4. Airway Cells Preparation for HRTEM and EDX analyses

Airway cells obtained from five non-frozen BALF samples were centrifuged (1500 g/10 min) and fixed with 2% glutaraldehyde in 0.1 M, pH 7·4 sodium cacodylate buffer, post-fixed in 1% osmium tetroxide in cacodylate buffer and put in 2% low-melting-point agarose and PBS for one hour at 4 °C. Cells were subsequently dehydrated with graded solutions of ethanol, impregnated with hexa-methyl-phosphor-amide, and embedded in EPON resin and 3% benzyl-dimethyl-amine. Cells were sectioned at 70 nm for TEM and 40 nm for HRTEM and EDX.

2.5. Vehicle Exhaust and Dust Collection and Preparation

Vehicle exhausts were collected with a cotton swab from the edges of car exhaust pipes. The exhaust samples were transferred into an Eppendorf tube and dispersed in 500 μL of distilled water. The suspensions were sonicated (10 min) and vortexed (1 min). 3 μL of each resulting suspension were then deposited onto grids and processed as described for the BALF extracts.

Dust was collected with a cotton swab near the vent on the inner part of the window roller shutters located on the second floor of a building situated by a national road in Antony (Southern suburb of Paris) or
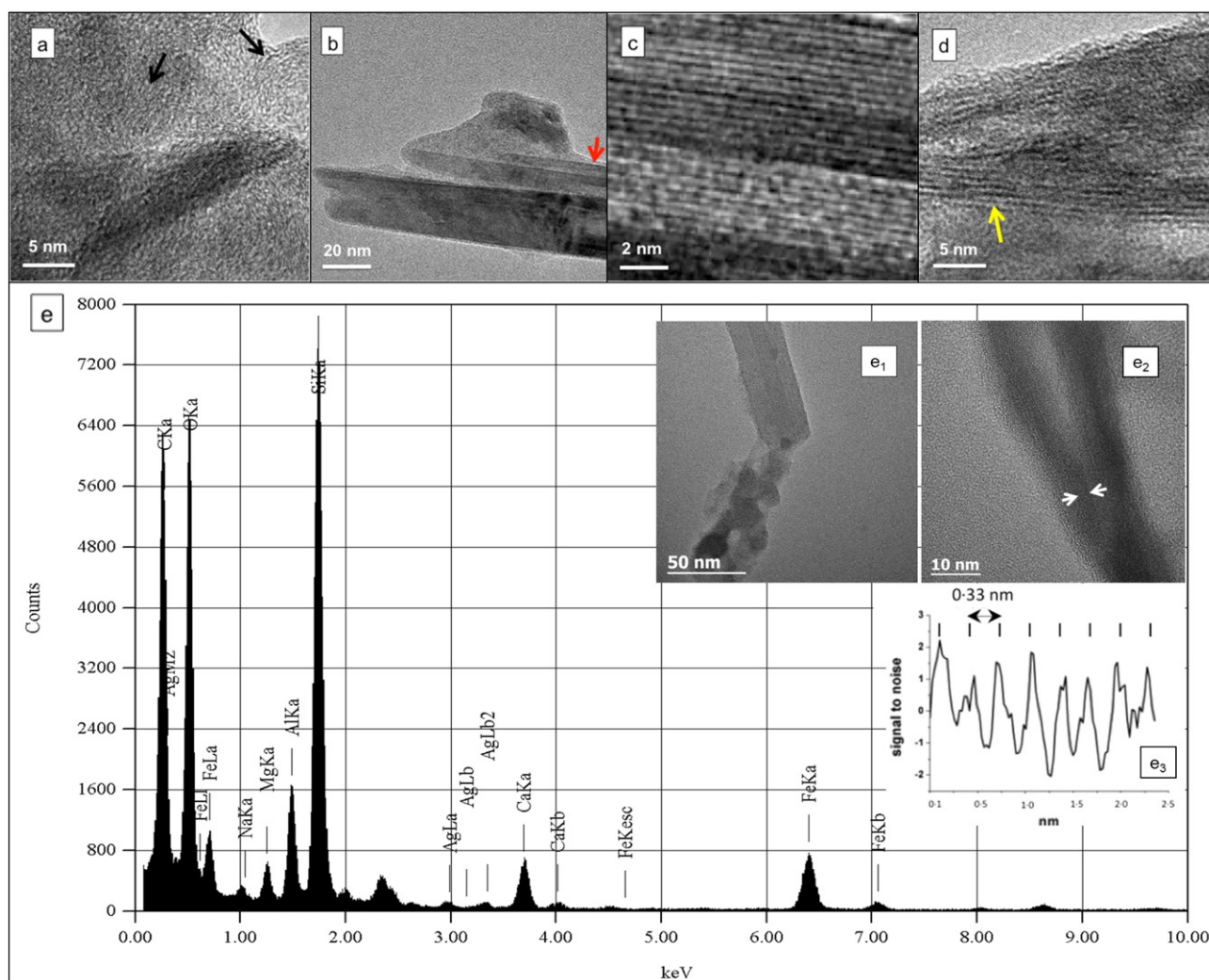

Fig. 2. HRTEM micrographs and EDX analysis of PM from Fig. 1. HRTEM of (a) nanospherules revealing amorphous carbon features, and of (b) CNT-like structures (Fig. 1, red arrows). (c) Magnified view of (b) revealing interlayer spacing characteristic of graphitic structures. (d) CNT-like structure (Fig. 1f, yellow arrows) showing interlayer spacing of 0.70 ± 0.02 nm. (e) Typical EDX spectrum and (e₁, e₂) HRTEM micrographs of nanospherules and CNT-like structures. As the substrate is an amorphous Si film, the carbon peak in the EDX spectrum arises exclusively from the sample. (e₃) Intensity profile measured between the two arrows in image (e₂) showing the characteristic interlayer distance (0.33 nm) of multi-walled carbon nanotubes.

located on the fifth floor in Nanterre (North Western suburb of Paris) near a residential, minor trafficked street. The samples were collected in July 2009 and July 2013 in households in flats with central heating but with no passive or active smoking. Dust samples were prepared and observed under the same conditions as the vehicle exhaust samples.

2.6. PM Characterization

Extracted PM from unfrozen BALF samples and PM inside the cells were first detected by TEM and then subjected to HRTEM, EDX, RS, and NIRFM for further characterization.

HRTEM and EDX analyses were performed with a JEOL ARM 200 F microscope operating at 80 kV (Ricolleau et al., 2013) and equipped with a CEOS aberration corrector, a cold field emission gun, and a JEOL EDX diode (JED 2300T). In order to detect carbon-rich regions, the analyzed samples were distributed on an amorphous silicon-coated TEM grid (SIMPore®).

2.7. Measurement of Interlayer Spacing

A statistician blindly analyzed the HRTEM micrographs with Image J software (NIH, Bethesda, USA) in order to measure the interlayer spacing of the nanostructures. The scale bar was set and fifteen lines were drawn perpendicular to the fringes. The "Plot profile" function was used to obtain a two-dimensional graph of the intensities of pixels along the linear selections. The graph was then processed with Microsoft Excel.

3. Results

3.1. Broncho-Alveolar Fluids Analysis

Firstly 64 randomly selected frozen BALF sample residues were retrospectively analyzed.

TEM micrographs of BALF extracts revealed a mixture composed mainly of aggregated PM and filament-like structures (Fig. 1a). While the filaments, corresponding to residual pulmonary surfactant, and most of aggregated material exhibited low electron density at high magnification, some nanostructures remained electron dense (Fig. 1b). At high magnification these nanostructures revealed the presence of aggregated carbon nanotube (CNT)-like structures (Fig. 1c) exhibiting diameters ranging from 10 to 60 nm and lengths of several hundred nm similar to those of synthetic multi-walled carbon nanotubes (MWCNTs) (Zhu et al., 2003). In order to investigate the origin of these structures, we analyzed vehicle exhaust and dusts deposited in Paris area.

3.2. Vehicle Exhausts and Dust Analysis

TEM analysis of the collected samples revealed three classes of particles (Fig. 1d–f): nano-spherules, MWCNT-like structures similar to those observed in the BALF extracts, and CNT-like bundles. The MWCNT-like structures were more abundant in the dust than in the vehicle exhausts. HRTEM (Fig. 2a–d) and EDX microanalyses confirmed the carbonaceous nature of both nano-spherules and MWCNT-like structures (>67% elemental carbon) (Fig. 2e).

HRTEM imaging revealed that, while the nano-spherules are mostly made of amorphous carbon (Fig. 2a), the MWCNT-like structures (Fig. 2b, c, e_1, e_2) exhibit two sets of alternating parallel white and black fringes, similar to those observed in synthetic MWCNTs (Zhu et al., 2003) corresponding to graphite layers periodically stacked as honeycomb (0002) planes oriented in a prismatic direction. The interlayer spacing of 0.33 ± 0.02 nm (Fig. $2e_3$) authenticates the presence of graphitic layers corresponding to actual MWCNT materials (and not just "CNT-like" materials) in the samples. On the other hand, some CNT-like structures (Fig. 2d) exhibited an interlayer spacing of $0.70 \pm$

0.04 nm ($n = 10$) suggesting the presence of single-walled carbon nanotube (SWCNT) bundles.

However, the presence of CNTs in BALF samples does not provide categorical evidence that CNTs penetrate deeply into the alveoli to reach lung cells. Indeed, at this stage, we have not observed CNTs inside intact cells because BALF sample freezing lyses the cells. Since CNTs were present in all examined BALF extracts, we hypothesized that the initial intact cells of the 64 BALF samples had contained CNTs so that intact cells in any fresh BALF sample should contain CNTs. To check this hypothesis, in a second step we examined intact cells extracted from five randomly selected (first to come) freshly collected BALF samples (without freezing) from another set of patients.

3.3. Lung Cells Examination

Optical microscopy after Diff-Quick staining and TEM revealed that all five unfrozen BALF samples contained several black-material-laden AM (Fig. 3) exhibiting the same features as those observed previously (Kulkarni et al., 2006). However, HRTEM analyses revealed that most black material was lamellar bodies (LBs) filled with oligo-lamellar surfactant layers (Schmitz and Muller, 1991) mainly composed of aggregates of branched or concentric layers of phospholipids (Fig. 3c, d).
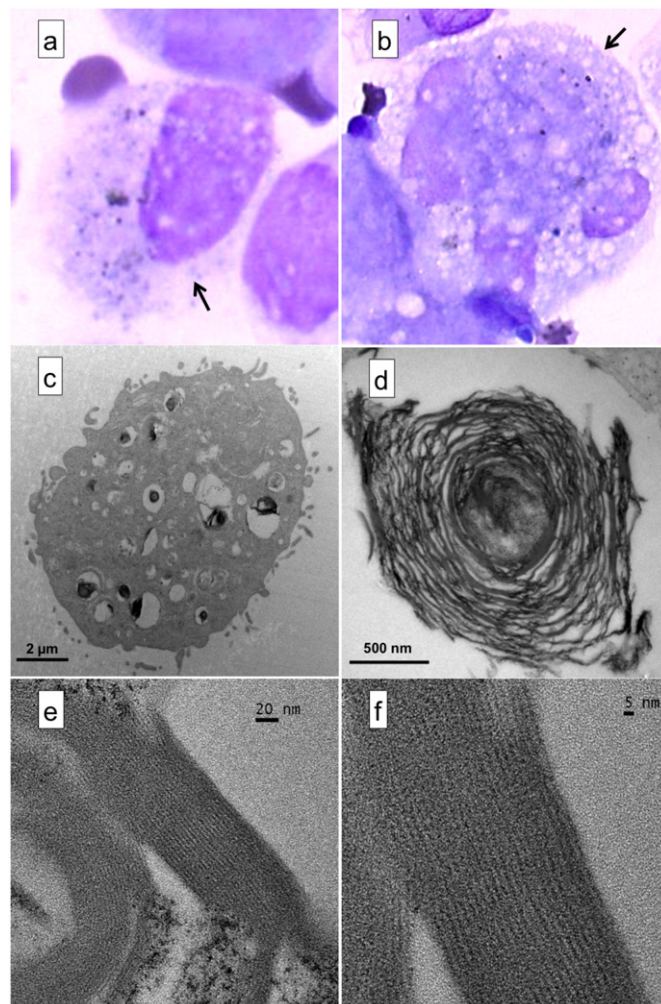

Fig. 3. Optical microscopy (OM), TEM, and HRTEM micrographs of lung cells from Parisian asthmatic children. (a, b) OM after Diff-Quick staining (magnification 100×) showing (arrows) lung cells containing black material. (c) TEM micrograph of a lung cell (likely type II pneumocyte) laden with black material mainly composed of lamellar bodies filled with concentric phospholipid layers of oligolamellar surfactant as evidenced by (d) TEM and (e, f) HRTEM of a black spot (the interlayer spacing is approximately 2 nm).
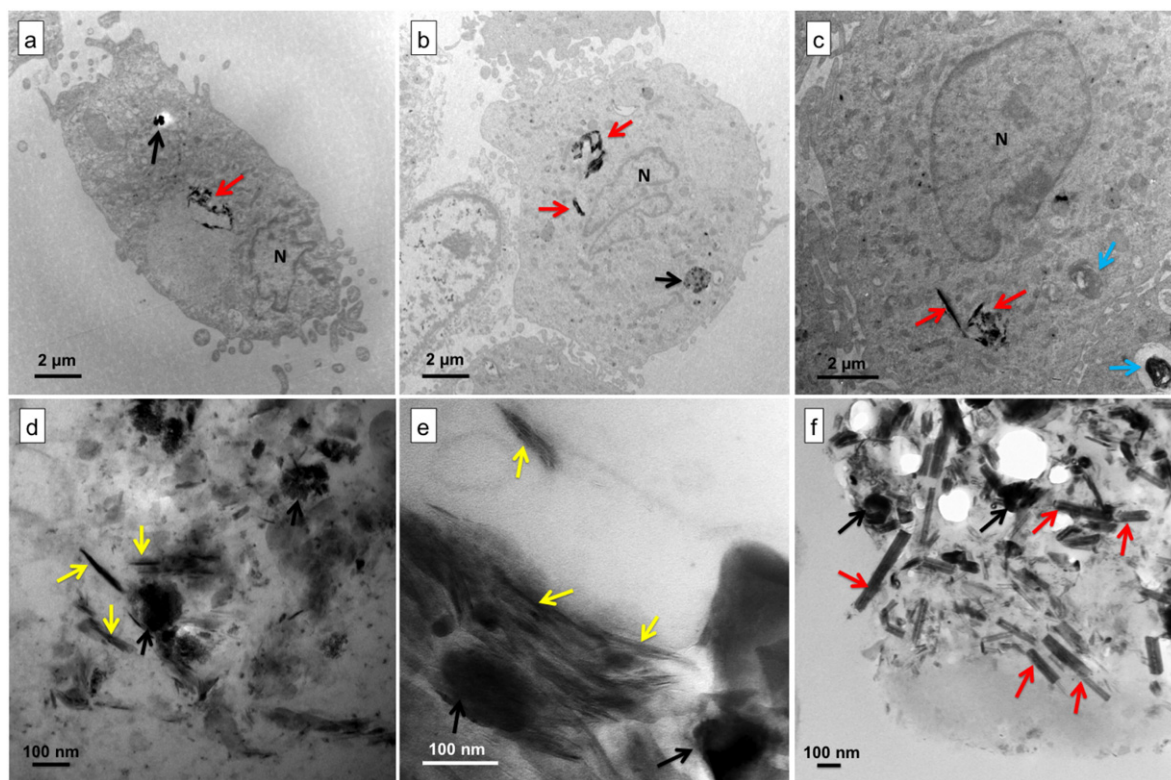
Fig. 4. TEM micrographs of lung cells. (a–c) Lung cell, probably an alveolar macrophage (N, nucleus) containing lamellar bodies (blue arrows) and PM (black arrows: nanospherules; yellow arrows: CNT-like bundles; and red arrows: MWCNTs,). (d–f) Magnification of (a–c). Note the similarity between the nanostructures observed inside the cells and in BALF extracts, dust, and vehicle-exhausts (Fig. 1).

Phospholipids cannot be mistaken for graphite layers because their interlayer spacing is approximately 2 nm (Fig. 3e, f).

Nevertheless, further TEM examination revealed the presence of PM-containing vacuoles (Fig. 4) inside some AM. Inside these vacuoles the observed PMs are similar to those we observed in dusts and vehicle exhaust samples, including nano-spherules, bundles of short and long nanotubes (Fig. 4c–e), and well-dispersed MWCNTs (Fig. 4f).

EDX analyses of PM inside the cells mainly exhibited a carbon signal (>95%), which confirms its carbonaceous nature (Fig. 5a). Inside the cells, dispersed MWCNTs also exhibited the MWCNT-characteristic interlayer spacing of 0.33 ± 0.02 nm. While short bundles were straight (Fig. 5a$_1$), long bundles were generally turned and twisted (Fig. 5a$_2$), which is probably due to growth defects (Zhu et al., 2003). The presence of CNTs inside the cells of five freshly collected BALF samples confirms our hypothesis and shows that CNTs penetrate lung cells of inhabitants in polluted areas.

Unlike LBs, which are mainly dispersed over large areas of lung cells (Fig. 3c), PMs were mostly found in isolated lysosomes of AM exhibiting only a few LBs (Fig. 4a–c). Table 1 summarizes the cell counts of the five freshly collected BALF. While the percentage of LBs-containing cells varied from 7.8 to 69.2% (median, 12.5%, n = 33 to 115 cells per BALF sample, median, 77 cells) of the examined cells, the percentage of CNT-containing cells varied from 1.3 to 7.8% (median, 7.0%) and the percentage of nano-spherules-containing cells varied from 2.1 to 7.7% (median, 3.9%). However, the size of PM observed inside the cells never exceeded 2 μm in diameter (Fig. 4), and they were impossible to distinguish from LBs by means of optical microscopy.

3.4. Near-Infrared Fluorescence Microscopy

To look for the presence of semi-conducting SWCNTs among the amounts of CNTs found in the BALF and cell samples, we have used NIRFM to scan five different AM samples. Only two of the five examined samples showed an NIR emission spectrum at all, although all five samples showed CNTs in both TEM and HRTEM micrographs. These samples exhibited multiple emissive spots that had significant excitation polarization dependence (>50% intensity change) (Fig. 5b–e), but only one sample exhibited NIR emission that completely disappeared with the changing of laser polarization (Fig. 5c), a phenomenon characteristic only of semiconducting SWCNTs (Cherukuri et al., 2004).

3.5. Raman Spectroscopy

Due to the scarcity and small sizes of the PM inside the cells, the signals obtained by Raman spectroscopy of several samples were very weak and non-informative.

4. Discussion

Among different indoor and outdoor combustion-derived airborne PM, carbonaceous particles represent an important fraction of pollutants (Cherukuri et al., 2004; Murr et al., 2004; Murr and Guerrero, 2006). These generally contain amorphous carbon, but, interestingly, may also contain carbon nanotubes (CNTs) and fullerenes (Murr et al., 2004; Murr and Guerrero, 2006; Lagally et al., 2012). Such findings suggest that humans may have always been exposed to CNTs. However, it is unknown whether, and to what extent, CNTs penetrate the lower respiratory tract.

In 2010 a study reported that CNTs were extracted from the lungs of the victims of the World Trade Center attack (Wu et al., 2010). However, this report cannot be generalized to environmental exposure. In addition, samples were only observed by low magnification TEM, which may not provide conclusive evidence, and CNTs were not visualized inside the cells.

To characterize CNTs, only a limited number of techniques are useful (Belin and Epron, 2005). Only HRTEM and scanning tunneling
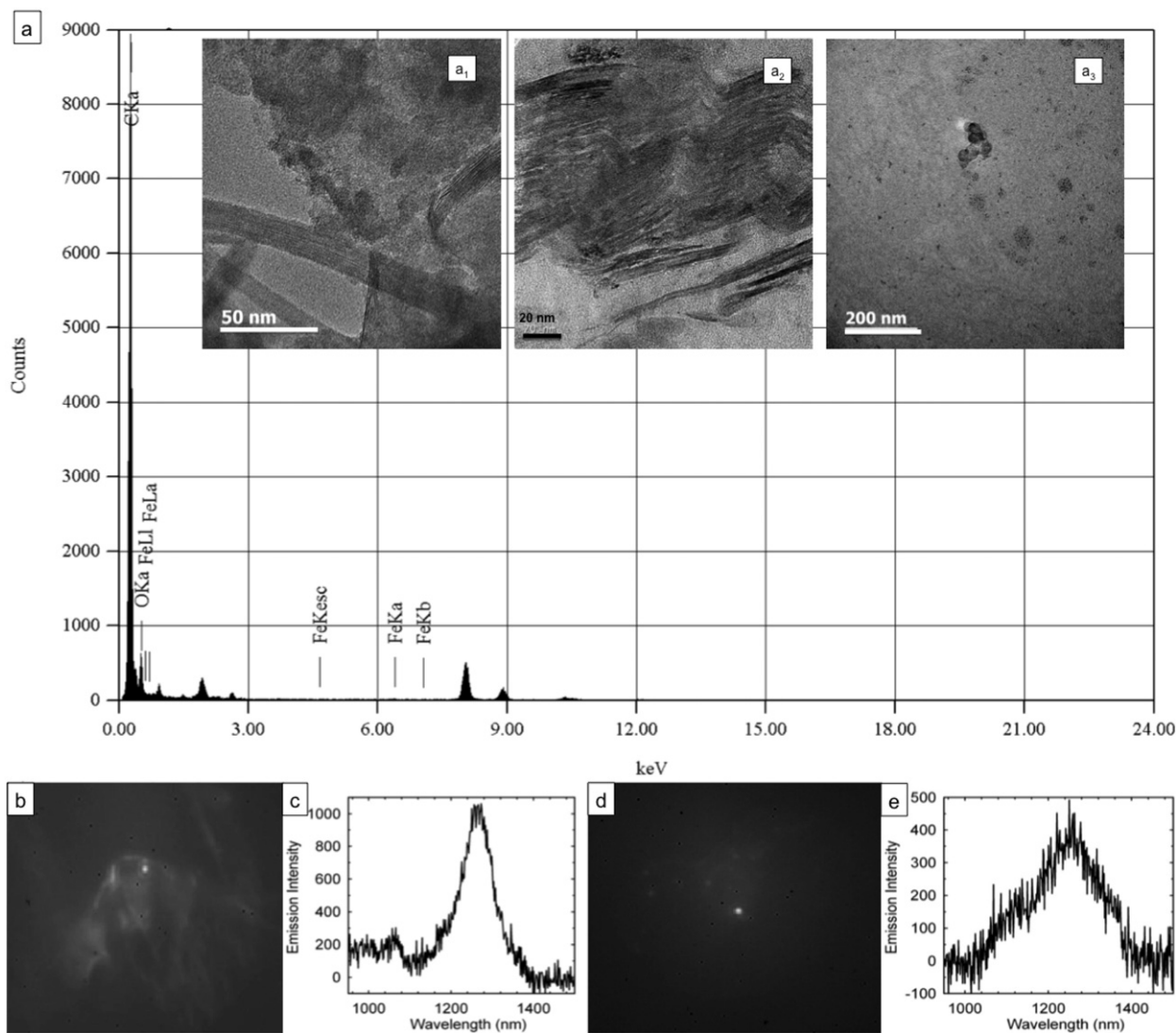
Fig. 5. HRTEM, EDX, and NIRFM analyses of PM inside lung cells, probably alveolar macrophages. (a) Typical EDX spectrum of (a₁–a₃) PM inside vacuoles (the absence of metal signals confirms the carbonaceous nature of these materials; the unlabeled peaks correspond to silicon from the HRTEM grid). (b, c) Bright-field image and NIR emission spectrum of a polarization-dependent SWCNT found in a BALF sample. (d, e) Bright-field image and broadened NIR emission spectrum of a CNT found in a lung cell. The sizes of the images in b and d are 50×70 μm.

microscopy are able to characterize CNTs at the individual level. EDX is needed to characterize the elemental composition of CNTs, while neutron and X-ray diffraction, NIRFM and Raman spectroscopy are global characterization techniques (Belin and Epron, 2005).

Here we used EDX, to assess the elemental composition of the PM found in broncho-alveolar lavage fluids and inside the cells of asthmatic Parisian children, and HRTEM was used to unambiguously characterize MWCNTs among these PMs.

PMs were first retrospectively assessed in 64 broncho-alveolar lavage fluid extracts by optical microscopy, TEM, HRTEM and EDX. To confirm these findings, the same techniques were prospectively used to analyze the PM observed inside the intact cells of 5 additional freshly collected BALF samples.

Taken together, our results show that PM is mostly composed of anthropogenic MWCNTs in all analyzed samples. These results also show that PM is impossible to distinguish from LBs by optical microscopy. Thus, results of previous studies, where carbon content of AMs was assessed by optical microscopy only (Kulkarni et al., 2006; Brugha et al., 2014), need to be reconsidered. TEM can be used to detect CNT-like structures, but this demands a highly trained person.

In order to look for the presence of some SWCNTs among CNTs found inside the cells, we also used NIRFM. NIRFM data were positive for two of the five examined fresh BALF samples. Although only individualized semiconducting SWCNTs are NIRF emissive (Cherukuri et al., 2004), these observations strongly support the presence of SWCNTs in some of the samples.

Although the number of examined samples is limited, the detection of CNTs in human samples presented in this study is significant because: 1) CNTs were present in all randomly selected samples, and 2) the MWCNTs observed in the lungs of Parisian children are similar to those detected in dust and vehicle exhaust samples collected in the Parisian area as well as to synthetic MWCNTs (Zhu et al., 2003), to MWCNTS found in ambient air samples collected in El Paso and Houston (USA) (Murr et al., 2004; Murr and Guerrero, 2006), and those trapped in domestic spider webs in Kanpur (India) (Sonkar et al., 2009).

Dusts were first collected near high-traffic roads. We observed no obvious correlation between the amounts of CNTs found in BALF samples with the distances of children's households from these roads: these amounts were comparable for children who lived the farthest (15 km) and those who lived the closest (1.5 km). Furthermore, the

Table 1
BALF cell counts.

Patients	1	2	3	4	5
Age (months)	58	23	30	13	12
Cells/mL	170,000	680,000	240,000	410,000	400,000
Macrophages (%)	88	52	56	78	60
Lymphocytes (%)	8	12	17	15	13
Neutrophils (%)	1	36	27	7	23
Eosinophils (%)	3	0	0	0	4
Siderophages (%)	0	0	0	0	0
Number of observed cells (by HRTEM)	115	48	80	33	77
Number of lamellar bodies containing cells[*]	37	5	10	9	6
Lamellar bodies containing cells (%)	32.2	10.4	12.5	69.2	7.8
Number of CNTs containing cells[*]	8	1	1	1	6
CNT containing cells (%)	7	2.1	1.3	7.7	7.8
Number of carbon nanospherules containing cells[*]	3	1	5	1	3
Carbon nanospherules containing cells (%)	2.6	2.1	6.3	7.7	3.9

[*] Determined by High Resolution Transmission Electron Microscopy (HRTEM).

dusts collected near very low-traffic roads contained impressively high amounts of carbon nanoparticles quite comparable to those found near high-traffic roads.

Since CNTs from anthropogenic sources may be present in indoor and outdoor air, and since air pollutants may be transported via the atmosphere, we expect that humans routinely breathe such carbon nanoparticles. While TEM has previously been used to detect carbonaceous particles inside human cells (Bunn et al., 2001), the authors only detected some carbon nano-spherules similar to those we observed. This is probably due to the fact that CNTs were not expected at the time. To the best of our knowledge, this is the first study showing that CNTs from anthropogenic sources reach human lung cells.

It is now well established that long MWCNTs (Poland et al., 2008), as well as large CNT-aggregates of short CNTs (Kolosnjaj-Tabi et al., 2010), can induce granuloma formation in animal models. At this stage, the sizes of CNTs we observed are not large enough to induce such granuloma formation. However, it is also well established that CNTs due to their large specific surface and chemical characteristics can adsorb a large variety of substances from gases and metals to large and small molecules (Ren et al., 2011). Thus, they may act as efficient vectors for air pollutants.

In addition, we wish to emphasize that in contrast to previous studies (Kulkarni et al., 2006) the main objective of this work was to characterize the PM found in the lungs of Parisian children and not to establish any link between the presence of PM in the BALF samples and the asthma condition of the examinees. Due to low concentrations of PM inside the cells it is impossible, at this time, to accurately quantify the carbon content of the lung cells.

Alveolar macrophages phagocytosis may be impaired in asthmatic patients (Brugha et al., 2014) (i.e. the loading of CNTs seen in this population may be less than for normal children), and asthmatic persons may have an altered deposition pattern. Besides, children deposition pattern may significantly differ from the adult ones. Thus, if CNTs are present in all examined BALFs from asthmatic children they should be present in healthy persons who have less difficulty in breathing. Thus, it is reasonable to conclude that modern humans are being routinely exposed to airborne CNT materials derived from anthropogenic sources.

5. Conclusions

We show here that CNTs are the main component of inhaled PM. We also show that PMs inside the cells are impossible to distinguish from lamellar bodies by optical microscopy alone. This strongly suggests that previous studies, linking the carbon content of airway macrophages and the decline of lung function, should be reconsidered.

Our data show that in order to detect carbon nanoparticles in a biological or an environmental sample; first it is necessary to use TEM in order to localize the suspected entities. Then EDX must be used to confirm the elemental composition. To identify MWCNTs among carbon nanoparticles, it is necessary to use HRTEM to measure interlayer distances. Finally, NIRFM is the most appropriate method to identify semiconducting individualized SWCNTs.

The scarcity of the observed PMs inside the cells is in line with recent reports showing that long-term exposure to fine particulate air pollution was associated with adverse health effects, even within very low concentration ranges (Beelen et al., 2014). Although the toxicity of carbon nanotubes is still a matter of debate, it is well established that long carbon nanotubes (Poland et al., 2008) and large aggregates of short ones (Kolosnjaj-Tabi et al., 2010) can induce a granulomatous reaction. Based on asbestos-like pathogenicity, it is believed that bio-persistent fiber-shaped nanomaterials that deposit in the lungs can cause oxidative stress and inflammation and could translocate to the pleura, ultimately leading to fibroplasia and neoplasia in the lungs and the pleura (Guarnieri and Balmes, 2014). Current research suggests that fibrous shape of carbon nanotubes could elicit effects similar to asbestos (Guarnieri and Balmes, 2014). Although the size of the observed carbon nanotubes inside lung cells at this time is not large enough to induce granuloma formation, their presence urgently requires more information on their fate and toxicity.

Authors' Contributions

J.K.T., K.B.H, S.B., D.A., L.J.W., and F.M. performed research and analyzed the data.

J.J. and L.Y. managed asthmatic children and collected BALF samples.

F.M. designed the research. J.K.T., L.J.W., H.S., and FM wrote the paper.

All authors discussed the results and commented on the manuscript.

Declaration of Interests

We claim that none of the authors has any conflict of interest.

Role of Funding Source and Ethics Committee Approval

Funding

Acknowledgment

References

Beelen, R., Raaschou-Nielsen, O., Stafoggia, M., Andersen, Z.J., Weinmayr, G., Hoffmann, B., et al., 2014. Effects of long-term exposure to air pollution on natural-cause mortality: an analysis of 22 European cohorts within the multicentre ESCAPE project. Lancet 383 (9919), 785–795.

Belin, T., Epron, F., 2005. Characterization methods of carbon nanotubes: a review. Mater. Sci. Eng. B 119 (2), 105–118.

Brugha, R., Mushtaq, N., Dundas, I., Mudway, I., Sanak, M., Grigg, J., 2014. Phagocytosis of fossil fuel particulates by macrophages in children with asthma. Lancet 383, S29.

Bunn, H.J., Dinsdale, D., Smith, T., Grigg, J., 2001. Ultrafine particles in alveolar macrophages from normal children. Thorax 56 (12), 932–934.

Cherukuri, P., Bachilo, S.M., Litovsky, S.H., Weisman, R.B., 2004. Near-infrared fluorescence microscopy of single-walled carbon nanotubes in phagocytic cells. J. Am. Chem. Soc. 126 (48), 15638–15639.

Gordon, S.B., Bruce, N.G., Grigg, J., Hibberd, P.L., Kurmi, O.P., Lam, K.-bH., et al., 2014. Respiratory risks from household air pollution in low and middle income countries. Lancet Respir. Med. 2 (10), 823–860.

Guarnieri, M., Balmes, J.R., 2014. Outdoor air pollution and asthma. Lancet 383 (9928), 1581–1592.

Just, J., Fournier, L., Momas, I., Zambetti, C., Sahraoui, F., Grimfeld, A., 2002. Clinical significance of bronchoalveolar eosinophils in childhood asthma. J. Allergy Clin. Immunol. 110 (1), 42–44.

Kelly, F.J., Fussell, J.C., 2012. Size, source and chemical composition as determinants of toxicity attributable to ambient particulate matter. Atmos. Environ. 60, 504–526.

Kolosnjaj-Tabi, J., Hartman, K.B., Boudjemaa, S., Ananta, J.S., Morgant, G., Szwarc, H., et al., 2010. In vivo behavior of large doses of ultrashort and full-length single-walled carbon nanotubes after oral and intraperitoneal administration to Swiss mice. ACS Nano 4 (3), 1481–1492.

Kulkarni, N., Pierse, N., Rushton, L., Grigg, J., 2006. Carbon in airway macrophages and lung function in children. N. Engl. J. Med. 355 (1), 21–30.

Lagally, C., Reynolds, C., Grieshop, A., Kandlikar, M., Rogak, S., 2012. Carbon nanotube and fullerene emissions from spark-ignited engines. Aerosol Sci. Technol. 46 (2), 156–164.

Li, C., Fang, D., Xu, D., Wang, B., Zhao, S., Yan, S., et al., 2014. Mechanisms in endocrinology: main air pollutants and diabetes-associated mortality: a systematic review and meta-analysis. Eur. J. Endocrinol. 171 (5), R183–R190.

Lim, S.S., Vos, T., Flaxman, A.D., Danaei, G., Shibuya, K., Adair-Rohani, H., et al., 2013. A comparative risk assessment of burden of disease and injury attributable to 67 risk factors and risk factor clusters in 21 regions, 1990–2010: a systematic analysis for the global burden of disease study 2010. Lancet 380 (9859), 2224–2260.

Murr, L.E., Guerrero, P.A., 2006. Carbon nanotubes in wood soot. Atmos. Sci. Lett. 7 (4), 93–95.

Murr, L.E., Bang, J.J., Esquivel, E.V., Guerrero, P.A., Lopez, A., 2004. Carbon nanotubes, nanocrystal forms, and complex nanoparticle aggregates in common fuel-gas combustion sources and the ambient air. J. Nanoparticle Res. 6 (2–3), 241–251.

Poland, C.A., Duffin, R., Kinloch, I., Maynard, A., Wallace, W.A.H., Seaton, A., et al., 2008. Carbon nanotubes introduced into the abdominal cavity of mice show asbestos-like pathogenicity in a pilot study. Nat. Nanotechnol. 3 (7), 423–428.

Pope, C.A., Burnett, R.T., Krewski, D., Jerrett, M., Shi, Y., Calle, E.E., et al., 2009. Cardiovascular mortality and exposure to airborne fine particulate matter and cigarette smoke shape of the exposure-response relationship. Circulation 120 (11), 941–948.

Raaschou-Nielsen, O., Andersen, Z.J., Beelen, R., Samoli, E., Stafoggia, M., Weinmayr, G., et al., 2013. Air pollution and lung cancer incidence in 17 European cohorts: prospective analyses from the European study of cohorts for air pollution effects (ESCAPE). Lancet Oncol. 14 (9), 813–822.

Ren, X., Chen, C., Nagatsu, M., Wang, X., 2011. Carbon nanotubes as adsorbents in environmental pollution management: a review. Chem. Eng. J. 170 (2), 395–410.

Ricolleau, C., Nelayah, J., Oikawa, T., Kohno, Y., Braidy, N., Wang, G., et al., 2013. Performances of an 80–200 kV microscope employing a cold-FEG and an aberration-corrected objective lens. Microscopy 62 (2), 283–293.

Samet, J.M., Gruskin, S., 2014. Air pollution, health, and human rights. Lancet Respir. Med. 3 (2), 98–100.

Schmitz, G., Muller, G., 1991. Structure and function of lamellar bodies, lipid-protein complexes involved in storage and secretion of cellular lipids. J. Lipid Res. 32 (10), 1539–1570.

Shah, A.S., Langrish, J.P., Nair, H., McAllister, D.A., Hunter, A.L., Donaldson, K., et al., 2013. Global association of air pollution and heart failure: a systematic review and meta-analysis. Lancet 382 (9897), 1039–1048.

Smith, K.R., Samet, J.M., Romieu, I., Bruce, N., 2000. Indoor air pollution in developing countries and acute lower respiratory infections in children. Thorax 55 (6), 518–532.

Sonkar, S.K., Tripathi, S., Sarkar, S., 2009. Activation of aerial oxygen to superoxide radical by carbon nanotubes in indoor spider web trapped aerosol. Curr. Sci. 97 (8), 1227–1230.

Wu, M.X., Gordon, R.E., Herbert, R., Padilla, M., Moline, J., Mendelson, D., et al., 2010. Case report: lung disease in World Trade Center responders exposed to dust and smoke: carbon nanotubes found in the lungs of World Trade Center patients and dust samples. Environ. Health Perspect. 118 (4), 499–504.

Zemp, E., Elsasser, S., Schindler, C., Kunzli, N., Perruchoud, A.P., Domenighetti, G., et al., 1999. Long-term ambient air pollution and respiratory symptoms in adults (SAPALDIA study). Am. J. Respir. Crit. Care Med. 159 (4), 1257–1266.

Zhu, W., Miser, D., Chan, W., Hajaligol, M., 2003. Characterization of multiwalled carbon nanotubes prepared by carbon arc cathode deposit. Mater. Chem. Phys. 82 (3), 638–647.